THE GEOLOGICAL SOCIETY OF AMERICA®

Hydrogeologic Implications of a Fault Scaling Relationship in Bedrock Aquifers

MATTHEW C. FRY[1]

ABRAHAM E. SPRINGER

PAUL J. UMHOEFER

School of Earth Sciences and Environmental Sustainability, Northern Arizona University, P.O. Box 5694, Flagstaff, AZ 86011

Key Terms: ***Faults, Structure, Hydrogeology, Modeling***

ABSTRACT

Because faults in bedrock aquifers can act as conduits or barriers to groundwater flow, defining their length and geometry is important for hydrogeologic investigations. The purpose of this study was to determine fault lengths through the use of a length versus displacement fault scaling relationship. Analytical, statistical, and field methods were used to define this relationship and to identify and evaluate outliers, which were then examined for refinement of their length and displacement. This study resulted in redefining the length for 5 of the 80 normal faults evaluated within a structural domain in the Transition Zone physiographic province of Arizona. Three faults with partially concealed or queried surface traces had their lengths decreased to values closer to the expected value, based on the determined length versus displacement relationship, using analytical and statistical methods. One fault had its length extended, and one fault was divided into two segments, based on the length versus displacement relationship as determined through field investigation. Newly determined fault lengths were incorporated into a digital hydrogeologic framework model of the regional aquifer, which supplies the water for the headwaters of the Verde River in central Arizona. This fault scaling technique can be applied in numerous settings, requiring minimal time and expertise, to better constrain fault lengths and possibly fault geometries. The critical assumptions of the method are that there are numerous faults of known length and that the fault array is largely similar in the rocks the faults cut, so that rheological differences are minimized.

[1]Corresponding author email: matt_fry@comcast.net.

INTRODUCTION

The concept of fault scaling of brittle faults has received much attention in the past two decades in the literature on structural geology. Investigators from numerous disciplines within geology have endeavored to fit the concept to their own individual applications. To further define how faults are formed and grow, structural geologists have been concerned with developing relationships for displacement versus fault length, width of fault damage zone versus fault length, or displacement versus width of damage zone (Walsh and Watterson, 1988; Cowie and Scholz, 1992a, 1992b). Schlische et al. (1996) demonstrated that there is no significant change in the linear displacement versus length relationship over more than eight orders of magnitude. Hydrogeologists have used the tendency of faults to follow a fractal distribution to quantify connectivity in faulted settings (Bour and Davy, 1997). Petroleum geologists use fault scaling relationships to estimate the density of faults below seismic resolution (Gauthier and Lake, 1993).

Depending on the age of the fault, intervals between activity, depth, type of materials faulted, development of gouge, and thickness of the fault core and damage zone, faults have the ability to act as either barriers or conduits to fluid flow (Bense et al., 2003; Shipton et al., 2005). Because of these important properties, correctly defining the length of faults is critical to characterizing the hydrogeologic setting of a heavily faulted region. This study focused on using analytical, statistical, and field methods to determine fault lengths and hence their potential connectivity to surrounding faults as a measure of determining their potential as conduits for groundwater flow.

The methods in this study were applied to a structural domain in the Transition Zone physiographic province of north-central Arizona. The Transition Zone is a relatively low-strain extensional

region dominated by normal faults. This study focused on defining a linear length versus displacement fault scaling relationship, where displacement is the maximum vertical displacement (throw), and length is the maximum two-dimensional trace length. Displacement is accumulated throughout the active life of a fault; the maximum value of which is usually found near the center of a fault. Displacement on a single fault surface ideally decreases to zero in all directions, except where the fault intersects a free surface or where displacement is transferred to a splay or to an intersecting fault (Walsh and Watterson, 1988). The methods described here should be transferable to similar extensional domains in other regions. Hypothetically, because the fault scaling relation holds for all types of faults (Schlische et al., 1996), these methods may apply broadly to other structural domains with contractional and strike-slip faults as well.

DESCRIPTION OF STUDY AREA

The fault scaling relationship of this study was applied in a specific aquifer with important regional implications. The upper Verde River is one of the largest remaining free-flowing perennial rivers in the southwestern United States. The headwaters region of the Verde River occurs at the intersection of a diverse geological terrain, where both regional bedrock and basin-fill aquifers contribute to the springs that form the base flow of the upper Verde River. The Verde River headwaters lie within the Transition Zone geographic and geologic province. The Transition Zone is a 60- to 100-km-wide boundary that separates the relatively stable and high Colorado Plateau to the north from the extended and low Basin and Range province to the south. Horst-block mountain ranges, corresponding graben and half-graben basins, volcanic-topped mountains, and steep canyons characterize the topography of the Transition Zone (Hendricks and Plescia, 1991).

During Late Cretaceous and early Cenozoic time, the Laramide Orogeny caused extensive deformation throughout central and southern Arizona (Dickinson, 1989). The Transition Zone was regionally topographically high but not intensely deformed. In the Oligocene to Miocene Epochs, the region changed to extensional deformation and renewed magmatic activity (Spencer and Reynolds, 1989). The Transition Zone lies immediately north of the highly extended part of the Arizona Basin and Range, but it is less extended than the Basin and Range, with relatively widely spaced large faults of moderate (few kilometers) offset (Spencer et al., 2001).

Paleozoic rock units of moderate hydraulic conductivity lie unconformably on the low-hydraulic-conductivity Proterozoic crystalline basement rocks. The middle Paleozoic Martin Formation and Redwall Limestone, which are dolomite and limestone units, respectively, form the regional bedrock aquifer. Definition of the extent of faults and associated fractures within the Paleozoic carbonate aquifer is important because fractures commonly provide the most significant effective porosity and permeability in carbonate aquifers (Mayer and Sharp, 1998), where dissolution commonly occurs along fractures, enlarging apertures, and resulting in large conduits for groundwater flow (Cook, 2003). The interconnectivity of the fracture and conduit systems often determines the extent of regional groundwater flow systems in carbonate aquifers (Mayer and Sharp, 1998).

Regionally, the major structural features include tight folds, shear zones, and strike-slip faults produced by major deformation during the Proterozoic (Krieger, 1965). Normal faults, monoclines, and gentle folds were produced by less severe deformation during Cretaceous to Cenozoic time. The Limestone Canyon Monocline (Figure 1), exposed on Big Black Mesa, is believed to be of Laramide age because of its similarity in structural style to monoclines on the Colorado Plateau (Davis, 1978). A smaller north-trending monocline along Bull Basin Canyon (Krieger, 1965) is probably also a Laramide-age structure. The Bull Basin Monocline (Figure 2) is overlain by undeformed Tertiary basalt and is therefore older than about 10 Ma (DeWitt et al., 2005). Northwest-striking normal faults with displacement down to the southwest formed between the monoclines during the Basin and Range extensional event in the Neogene.

High-angle normal faults are largely responsible for the modern geomorphology of much of the Basin and Range province of Arizona, and to a lesser extent, the Transition Zone, including the study area. The study area is located at the southeastern end of the Big Chino fault (Figure 2), a northwest-striking, southwest-dipping normal fault that is an active late Cenozoic structure. The study area is also in the gap or step-over area between the Big Chino fault and the northwest-striking, northeast-dipping Verde fault (Figure 1). The step-over area has many normal faults of varying orientations. Approximately three-quarters of the faults present in the Verde River headwaters strike northwest and are aligned perpendicular to the principal direction of Cenozoic extension. The remaining faults strike in various other orientations. The minimum displacement and length values for faults used in this study are 2 and

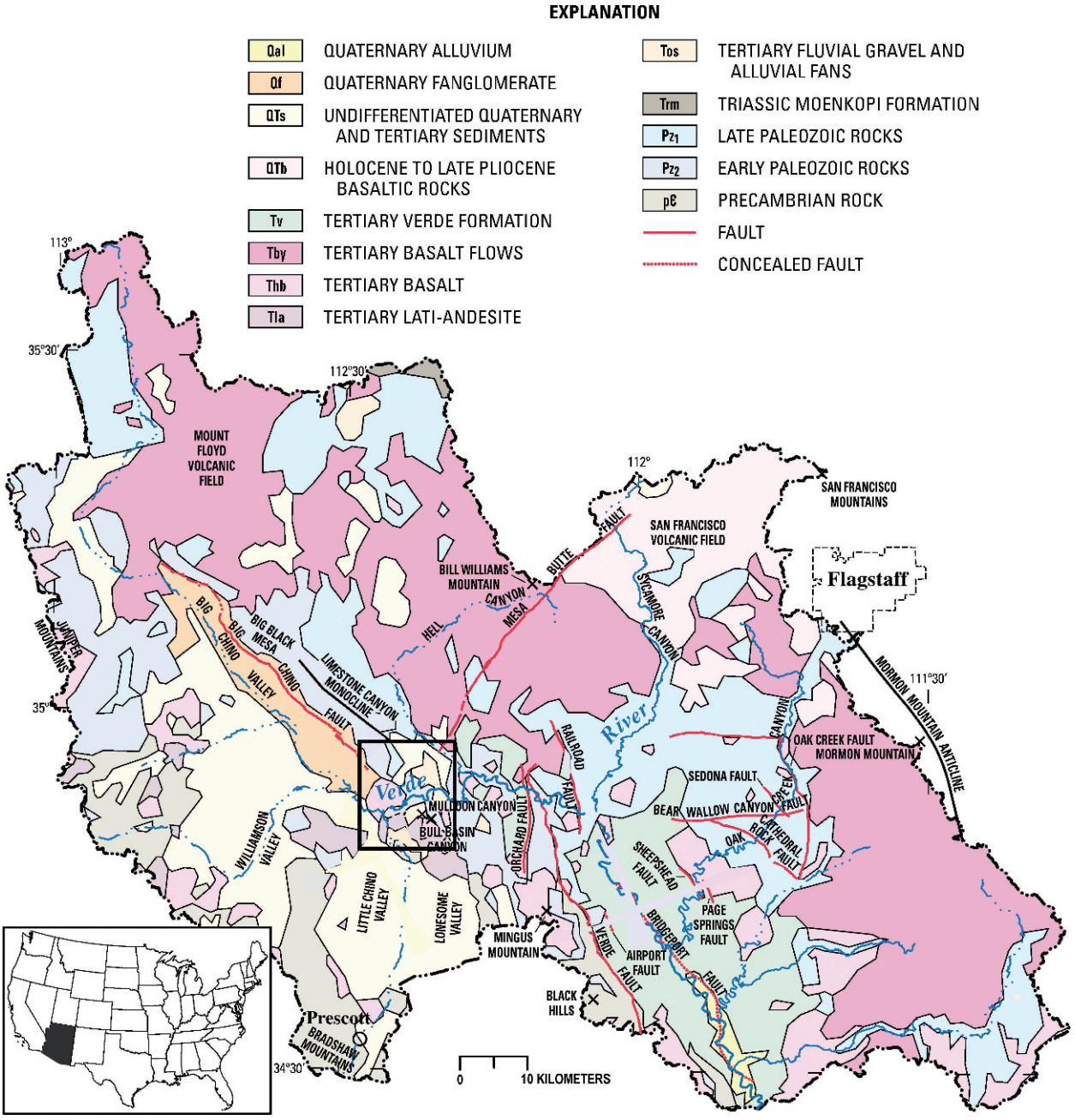

Figure 1. Generalized geology and structures of the upper and middle Verde River watersheds (modified from Blasch et al., 2006). Study area is shown with black box. See inset map for location.

120 m, respectively; maximum displacement and length values are 170 and 7,400 m, respectively.

The presence of normal faults, and their density in some locations within the Verde River headwaters, has led researchers to note their role in the hydrogeologic system (Wirt et al., 2005). In particular, spring locations within the Verde River canyon directly correlate with the locations of individual faults or clusters of faults based on field observations made by the authors. Most exposures of these faults are within the canyon walls, as the canyon rims are extensively covered by Tertiary basalt. Where exposed, the faults generally show only minimal development of mineralized breccia, usually approximately 1 ft thick or less. There are no data available for hydraulic conductivity of any of the faults in the study area. However, there is no indication that the faults are acting as zones of lower hydraulic conductivity than the surrounding bedrock, as would be suggested by differential head elevations across the faults. The combination of factors described here, and the potential for dissolution along fractures in

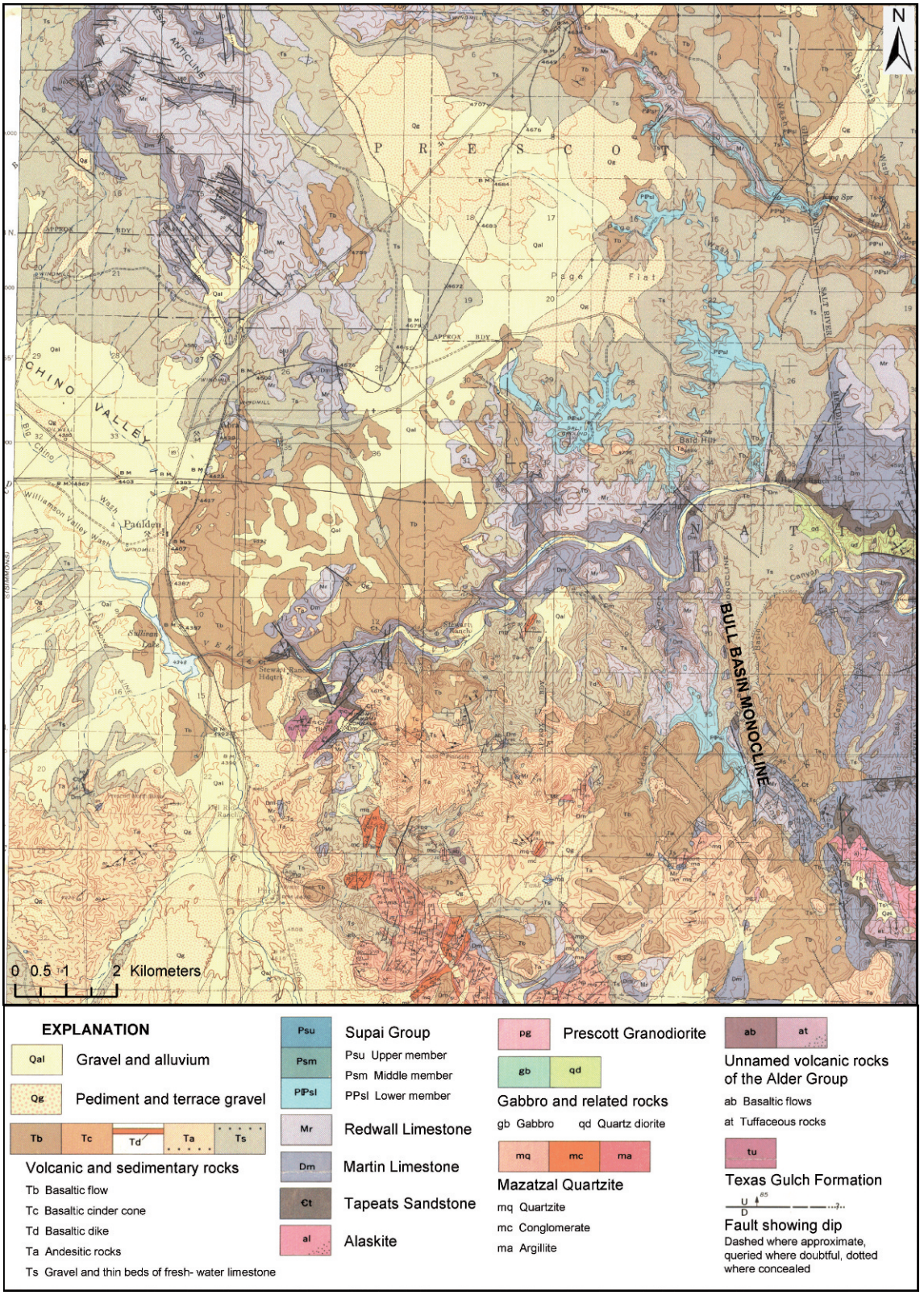

Figure 2. Geologic map of Verde River headwaters study area (modified from Krieger, 1965).

carbonate rocks, suggests that locally faults, or at least the fractures associated with them, are acting as conduits. The role of faulting in the regional groundwater system is unknown, predominantly because fault interconnectivity is unknown. Faults or fault clusters within the study area have been mapped as isolated structures (Krieger, 1965), but uncertainty exists in the mapping due to locally poor exposure. This study serves to define the potential linkage as conduits between individual faults or fault clusters by refining their mapped lengths where exposure is poor. Therefore, the spatial distribution of faults is used as a proxy for the potential spatial distribution of increased hydraulic conductivity zones associated with them.

The methods applied in this study can be used in areas dominated by either compressional or extensional tectonics, or both, as in the case of this study. If the area has been deformed by more than one tectonic event, identifying and separating faults based on age and tectonic influence are important, because displacement versus length ratios are potentially affected by age and tectonic setting. Secondary thrust faults associated with monocline development during the Laramide Orogeny were not evaluated in this study, and the data set contains only normal faults.

METHODS

A geologic map of the study area (Krieger, 1965) (Figure 2) was scanned and imported into ArcGIS (Environmental Systems Research Institute, 2004), along with U.S. Geological Survey (USGS) 7.5′ quadrangle 10-m resolution digital elevation models (DEMs) downloaded from the Geocommunity website (Geocommunity website, 2006). A 15-m (50-ft) contour interval of the DEMs was generated, matching that of the geologic map. The existing geologic map was georeferenced by matching USGS map contours to those generated from the DEMs. Overlaying the geologic map onto the mosaicked DEMs in ArcGIS allowed for accurate elevation to be determined at any location on the geologic map. Elevations of stratigraphic contacts on opposing sides of a fault were determined and used for calculation of vertical displacement of the fault (throw). Displacement and length values derived from the geologic map (Krieger, 1965) were plotted in Microsoft Excel (Figure 3). By convention, displacement versus length graphs are plotted on a log-log scale. To simplify statistical analysis, the log of the values was plotted on an arithmetic scale, which results in an identical data distribution. The amount of scatter present in the data set from this study is typical of the scatter in data sets used by other researchers (Schlische et al., 1996) (Figure 3).

Fault scaling relationships within the Verde River headwaters were determined using a reduced major axis (RMA) linear analysis (Davis, 2002). The RMA of the 80 faults within the study area was calculated using the following equations:

$$b1 = Sy/Sx \tag{1}$$

$$b0 = (\text{mean } y) - b1 \times (\text{mean } x) \tag{2}$$

where $b1$ is the slope of the RMA, $b0$ is the y-intercept of the RMA, Sy is the standard deviation of y (0.42), Sx is the standard deviation of x (0.39), (mean y) is the mean y-value (2.85), and (mean x) is the mean x-value (1.23). The resulting RMA line has a slope of 1.06 and a y-intercept of 1.54 (Figure 3). Standard deviation and mean values were calculated in Microsoft Excel.

The simple elastic model for faulting dictates that displacement and length should have a linear relationship, and therefore a line fit to the data on a log-log plot should have a slope of one (Cowie and Scholz, 1992a, 1992b). The presence of outliers within the data set caused the slope of the linear regression line to be approximately 0.65, i.e., a poor fit. Simple linear regression analysis assumes that one variable is dependent on another. In a relationship of fault displacement versus fault length, it is unclear which variable could appropriately be designated as dependent on the other variable. The RMA method has been used by other researchers for similar data sets (Bailey et al., 2005), and it does not require definition of a dependent and independent variable. Additionally, the RMA method, with a resulting slope of 1.06, obtained a much better fit to the theoretical relationship developed by other researchers. The RMA method minimizes the product of the deviations from the fitted line in the x and y directions, equivalent to minimizing the area between a data point and the fit line (Figure 4). The r-squared value of the data set, 0.37, was calculated in Microsoft Excel and used to calculate the standard error of the slope and y-intercept of the RMA using the following equations:

$$Seb1 = b1 \times \sqrt{\frac{1-r^2}{n}} \tag{3}$$

$$Seb0 = Sy \times \sqrt{\frac{1-r^2}{n}} \times \left[1 + \frac{(\text{mean } x)^2}{Sx^2}\right] \tag{4}$$

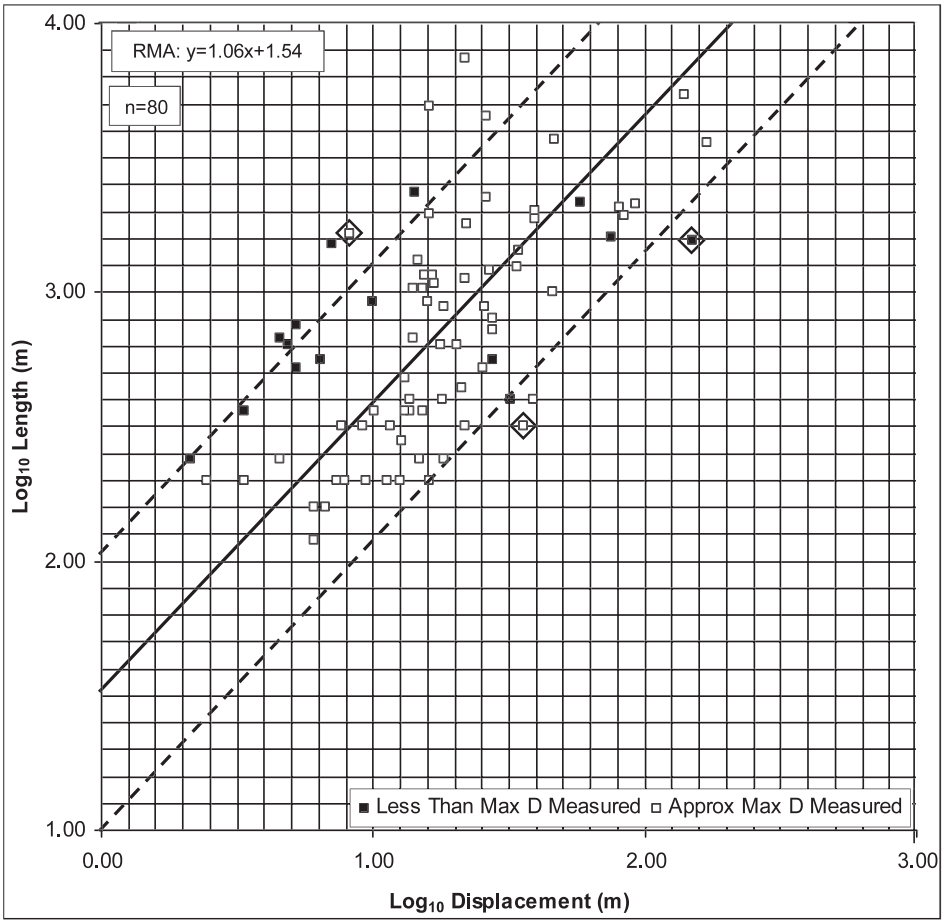

Figure 3. Log displacement versus log length of faults in the Verde River headwaters showing reduced major axis (solid line) and surrounding 80 percent confidence interval (dashed lines). Faults with displacement measurements approximately representing maximum displacement are shown with hollow squares. Faults with displacement measurements suspected to not represent maximum displacement, due to displacement measurement taken significantly off center, are shown with solid squares. Faults that were subsequently field checked are surrounded by diamonds.

where *Seb*1 is the standard error of the slope, *Seb*0 is the standard error of the *y*-intercept, r^2 is the *r*-squared value, and *n* is the number of values in the data set (80). The standard error of the slope is 0.09, and the standard error of the *y*-intercept 0.41. The standard error of the slope is not significant when compared to the standard error of the *y*-intercept, and so it was not incorporated into further calculations. The standard error of the *y*-intercept was used to calculate an 80 percent confidence interval around the RMA (Figure 3) to identify outliers, using the following equation:

$$(\text{mean } x) \pm z \times Seb0 \tag{5}$$

where *z* is the critical value associated with the desired level of confidence. The critical value of *z*, 1.28, correlates to a 90 percent and 10 percent cumulative probability, the difference between the values being 80 percent. An 80 percent confidence interval was selected as opposed to what may be considered a more traditional value of 90 percent because the 90 percent value identified very few outliers and did not include some faults that were suspect. The 80 percent confidence interval corresponds to an 80 percent

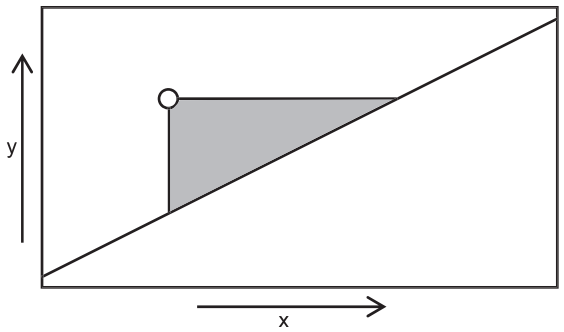

Figure 4. Reduced major axis calculation minimizes the product of deviations in the *x* and *y* directions, equivalent to minimizing area of the shaded triangle (after Davis, 2002).

Table 1. *Results of evaluating faults outside of the 80 percent confidence interval of the RMA in the Verde River headwaters.*

Fault	Relationship[1]	Potential Reason	Method	Action
40	L >> D	Incorrectly mapped L	Field	Reassign L
41	L >> D	Measured D not max D	GIS	None
44	L >> D	Measured D not max D	GIS	None
54	L >> D	Incorrectly mapped L	GIS	Reassign L
55	L >> D	Incorrectly mapped L	GIS	Reassign L
60	D >> L	Incorrectly mapped	Field	None
71	L >> D	Measured D not max D	GIS	None
72	D >> L	Interaction with adjacent faults	GIS	None
76	L >> D	Incorrectly mapped L	GIS	Reassign L
81	D >> L	Incorrectly mapped L or D	Field	Reassign L
82	L >> D	Measured D not max D	GIS	None
83	L >> D	Measured D not max D	GIS	None
93	D >> L	Interaction with adjacent faults	GIS	None

[1]Relationship identifier: L >> D, length too great for displacement; D >> L, displacement too great for length.

probability that another sample of faults from the same population would have a calculated RMA with a y-intercept between 1.02 and 2.06, the result of adding and subtracting 0.52 to the y-intercept, as calculated in Eq. 5.

RESULTS

Thirteen of the 80 faults, or 16 percent, had corresponding length and displacement values outside of the 80 percent confidence interval of the RMA (Figure 3). Faults that plotted outside of the 80 percent confidence interval were re-examined in ArcGIS. If a reason for the deviation could not be identified in ArcGIS, such as the presence of another fault nearby, a large portion of the fault mapped as concealed, or a displacement measurement that was taken significantly off center and therefore suspected to not represent maximum displacement, the faults were field checked. Results of re-examining faults in ArcGIS and field checking are shown in Tables 1 and 2. Table 1 lists the 13 faults outside of the 80 percent confidence interval of the RMA and potential reasons.

Table 1 also lists the method used to determine the reason the fault plotted outside of the 80 percent confidence interval of the RMA and what action, if any, was taken. Table 2 lists five faults that were reassigned new lengths based on the calculated scaling relationship, and it includes the length as originally mapped, the length as suggested by the RMA based on the displacement, and the assigned length.

Three faults required field checking because the calculated displacement versus length ratio did not correlate with the faults as mapped, and a reason could not be determined in ArcGIS from the digitized geologic map. Field checking entailed walking the mapped surface trace of the fault and beyond to ensure the length was mapped correctly, and taking numerous bedding attitude measurements on opposing sides of the fault to ensure local dip was not resulting in inaccurate displacement measurement. Displacement was measured directly from offset of unit contacts or determined using average thickness values of Paleozoic stratigraphic units and local dip.

Displacement of fault 81 (Tables 1 and 2) was determined to be accurate, but its mapped length was far too short for its corresponding displacement. Because evidence in the field suggested that the fault continued to the south, the fault was extended in this direction (red line on Figure 5A). The maximum displacement value was measured at the extreme north end of fault 81, as mapped (Figure 5A). Because maximum displacement does not usually occur at the end of faults (Schlische et al., 1996), the fault likely continues to the north as well. The fault was extended to the north (red line on Figure 5A), though its surface trace is coincident with a wash and concealed by Quaternary sediment, and its exact length could not be determined. Total displacement of fault 60 (Table 1) was determined to be accurate; however, the displacement is distributed approximately equally across four spatially close parallel faults. The faults were mapped (Krieger, 1965) as one fault (Figure 5B), which is appropriate for the

Table 2. *Results of reassigning lengths (L) of five faults in the Verde River headwaters.*

Fault	Mapped L (m)	RMA L (m)	Assigned L (m)
40	1,640	320	480/800[1]
54	7,400	1,080	1,080
55	4,520	920	920
76	4,920	680	840
81	760	7,080	3,520

[1]Fault was divided into two segments.

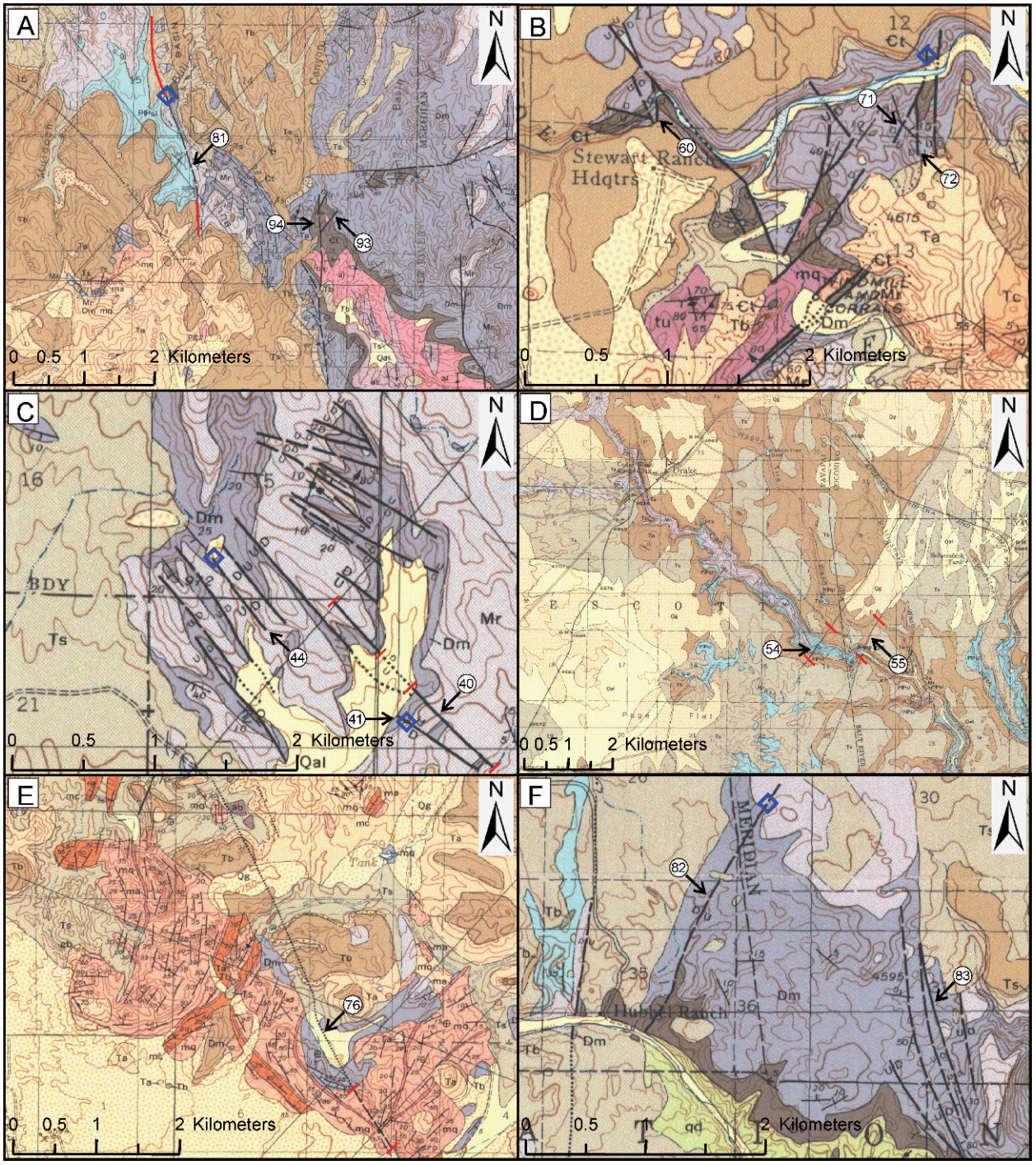

Figure 5. Geologic maps showing locations of selected faults in the Verde River headwaters (Krieger, 1965). (A) Fault 81's length was extended based on the calculated scaling relationship (red lines). Location of displacement measurement is shown with blue diamond. Fault 93 has a displacement value too great for its length, presumably due to interaction with fault 94. (B) Fault 60, represented as a single fault on the map, is actually four parallel faults. Fault 71 had its displacement measured significantly off center (blue diamond). Fault 72 has a displacement value too great for its length, presumably due to interaction with fault 71. (C) Fault 40, mapped as a single fault, is likely two discontinuous segments (red lines). Faults 41 and 44 had their displacement measured significantly off center (blue diamonds). (D) Faults 54 and 55 had their lengths decreased based on the scaling relationship (red lines). (E) Fault 76 had its length decreased based on the scaling relationship (red lines). (F) Fault 82 had its displacement measured significantly off center (blue diamond). Measured displacement of fault 83 is a minimum value, due to the absence of the Martin Formation and Redwall Limestone contact on the west side of the fault. See Figure 2 for explanation.

1:48,000-scale map, but because displacement is distributed across four smaller proximal faults, the displacement versus length relationship developed in this study is not valid for fault 60. Therefore, the length(s) of the fault(s) as mapped cannot be confirmed. The displacement of fault 40, on both sides of the concealed central portion (Figure 5C), was determined to be accurate as mapped, as were lengths of the unconcealed portions. It is our interpretation that the length of fault 40 is too short for its relative displacement because the fault has been incorrectly mapped as continuous, when it more likely represents two discontinuous segments. Based on this interpretation, the fault has been divided into two segments (Figure 5C).

Faults 54 and 55 were reassigned length values directly from the mean value suggested by the RMA, based on their displacement (Figures 3 and 5D and Table 2). The mean RMA value underestimated the length of fault 76 based on its displacement (Table 2), as determined by the length of its mapped surface trace (Figure 5E). Though a portion of the fault is mapped as concealed or queried, a portion of the fault's length is known, and this portion is longer than suggested by the mean RMA value. Fault 76 was reassigned a length value coinciding with the portion that is not concealed or queried (Figure 5E), and not directly from the RMA value corresponding to its displacement (Table 2). It is believed that the RMA underestimated the length of fault 76 because measured displacement does not represent maximum displacement. Faults 41 and 44 have displacements too small for their respective lengths. It is presumed that this results from their displacement being measured significantly off center (Figure 5C). Fault 71 also has too little displacement for its length, and it is hypothesized that this results from an off-center measure of displacement (Figure 5B). Faults 82 and 83 have displacement values too small for their respective lengths. Fault 82 was measured significantly off center, and displacement of fault 83 was known to be a minimum value, as the contact between the Martin Formation and Redwall Limestone is only present on the east side of the fault, and it has been removed by erosion on the west side of the fault, resulting in a minimum measured value of displacement (Figures 2 and 5F). Fault 72 has displacement too great for its length, which is presumably due to interaction with fault 71 (Figure 5B). Fault 93 also has too much displacement for its respective length. It is hypothesized that this results from interaction with fault 94 (Figure 5A).

Newly determined fault lengths were used in construction of a digital hydrogeologic framework model utilizing EarthVision, a three-dimensional (3-D) geologic GIS. EarthVision simulates faults as 3-D planar structures and allows for visual interpretation of fault network connectivity utilizing its 3-D Viewer. The refinement of the spatial distribution of faults, by utilizing a length versus displacement fault scaling relationship, generated constraints on potential groundwater flow paths. Because fault clusters were farther apart than the length of the longest fault contained in any cluster, fault clusters were determined to not be hydrogeologically connected. Redefining the lengths of five faults made the structural hydrogeologic relationships more accurate and discernable in the digital hydrogeologic framework model, and provided a conceptual model of the regional carbonate aquifer. These data can be used to generate a better understanding of the regional groundwater system, indicating that fault network interconnectivity likely has little influence on regional groundwater flow paths, and they can be incorporated into future groundwater modeling efforts.

DISCUSSION

Any number of potential complications can result in inaccurate displacement and/or length determinations. Errors in original mapping and/or the georeferencing process can result in inaccuracy. In our study, these errors are believed to be minimal due to the accuracy of the original map (Krieger, 1965) as checked in this study and the care taken in georeferencing, which matched topographic contours on the existing geologic map to those generated from the DEMs. Original mapping errors arise from incorrect interpretations, relatively poor exposure of faults and offset units, faulted units that are thicker than the offset, and a poor topographic base. Because the geological mapping for our study area was done in the mid-1950's, the current USGS 7.5-minute 1:24,000 topographic quadrangles were not yet available, and there are significant deviations between the topographic base that existed then and present topographic base maps. Many of the faults within the study area were field checked prior to this study. All fault locations that were field checked were determined to be accurate, and though not all faults were field checked, the level of confidence in the original map by Krieger (1965) is high. Other work by colleagues in the area confirmed the accuracy of the map by Krieger (Ronald Blakey, 2006, oral communication). The study area is a semiarid landscape in which much of the geology is well exposed, and therefore we gain further confidence in the accuracy of the faults.

Lithology can be an important variable in the scaling relationships of faults because the difficulty in

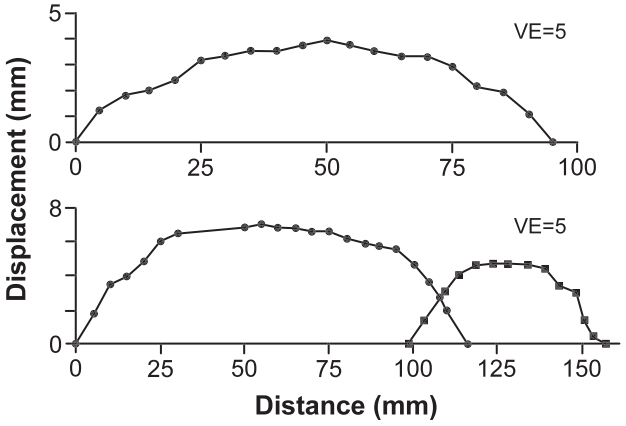

Figure 6. Displacement gradient with respect to length for an isolated normal fault (top), and linked fault system (bottom). Note that displacement gradients are higher at tips of linked faults (modified from Schlische et al., 1996).

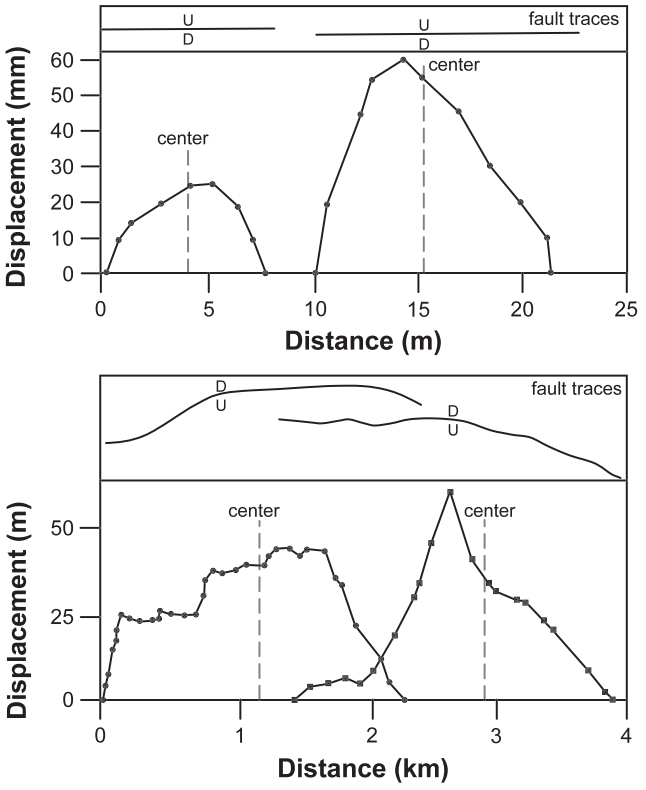

Figure 7. Effect on displacement gradient of under-lapping (top) and overlapping (bottom) faults (modified from Willemse et al., 1996).

initiating fault development and sustaining fault growth is influenced by rock-type–dependent properties such as intact rock strength and frictional strength (Walsh and Watterson, 1988; Cowie and Scholz, 1992a, 1992b). Approximately 90 percent of the faults examined in this study are exposed in Paleozoic carbonates, so lithologic variability is minimized. However, a few faults are in Tertiary volcanic rocks or Proterozoic crystalline rocks. In general, the area contains a relatively simple section with similar rock types throughout; therefore, the authors do not anticipate that lithologic variability was a significant factor in the scaling relationship.

Several other factors yield inaccurate displacement measurements. To ensure consistency within the data set, the desired displacement value to correlate with fault length is the maximum value of displacement (Bonnet et al., 2001). On isolated faults, this value is approximately located at the center of a normal fault (Schlische et al., 1996) (Figure 6). Because displacement may not be measurable at the central location due to concealment or lack of unit contacts or marker beds by which to measure displacement, something less than the maximum value is recorded, and error can result. This source of error is somewhat mitigated because simple normal faults have near-maximum displacement over approximately half of their length (Figure 6). Due to the limited number of faults in the study area for which numerous displacement measurements could be determined along the length of the fault, and inherent coarseness of displacement determinations due to discrepancies between the topographic base utilized by Krieger (1965) and current versions derived from DEMs, we have been unable to demonstrate displacement gradient with respect to length for any faults within the Verde River headwaters. However, no evidence exists to demonstrate normal faults in the study behave any differently than other normal fault populations reported in the literature (Schlische et al., 1996; Willemse et al., 1996; and Ferrill and Morris, 2001).

Some locations within the study area contain high densities of faults, such that interaction occurs, especially on Big Black Mesa (Figure 2). Fault interaction also affects the distribution and value of maximum displacement (Willemse et al., 1996) (Figure 7), increasing maximum displacement values, and shifting the maximum value from the approximate center of a fault toward the overlapping or under-lapping ends. Fault growth by segment linkage also affects the value and distribution of maximum displacement and can introduce scatter in displacement versus length data (Cartwright et al., 1995). When two isolated faults link, an initial increase in length is attained without a corresponding increase in displacement, as the low-displacement ends of two faults become the center of a new fault. The initial displacement deficit at the center of the linked fault is overcome with time, assuming the fault does not die soon after linkage. This results in a step-like growth pattern, as first length increases, and then displacement increases (Cartwright et al., 1995).

Relative age also affects displacement versus length ratios of faults. In general, faults that have been subjected to a longer duration of active faulting have a more developed damage zone, which is usually softer than the surrounding rock (Gudmundsson, 2004). In this manner, long-lived faults can display increasing displacement without a proportionally equivalent increase in length, and therefore the displacement versus length ratio can increase over time (Gudmundsson, 2004). This relation is present in the faults in the Verde River headwaters. Assuming length corresponds to relative age, because even if the displacement versus length ratio is increasing with time, length itself is still increasing, faults with greater lengths have been active for a longer period of time since inception. The longest 25 percent of faults in the study have a greater displacement versus length ratio, as evidenced by a shallower slope of the RMA, than that of the entire data set (Figure 8). Slope of the RMA for all faults in the study is 1.06, compared to 0.50 for the longest 25 percent of the faults in the study. The RMA of the longest 25 percent of faults in the study does not appear to fit as well as the RMA for all data; however, for consistency the same regression method was employed.

Only faults for which some of the surface trace was mapped (Krieger, 1965) as concealed or queried were reassigned a new lower length value closer to the mean value suggested by the RMA without field checking. Faults in which displacement values were determined distal from the center of the fault, and which had displacement values too low for their corresponding length, were assumed to not represent maximum displacement. Therefore, original length was assumed to be correct, and no action was taken. Faults for which displacement values were believed to be accurate, but which were too high for their corresponding length values, were examined to see if fault interaction could be influencing the measured displacement value. Faults that were near other faults with similar dip orientations, and which displacement values too high for their respective lengths, were assumed to be affected by adjacent faults, and no action was taken. Faults deemed incorrectly mapped with respect to length or displacement may be incorrect, or local attitude of bedding may be resulting in inaccurate displacement determinations. These faults were investigated in the field to determine the source of error, and numerous measurements of bedding were taken proximal to the fault.

Isolated clusters of faults are located throughout the Verde River headwaters (Figure 2); however, these isolated clusters show no evidence of connectivity to other fault clusters. Based on field observations, spring locations do correlate to locations of faults or clusters of faults. Based on the displacement versus length relationship calculated in this study, the faults do not appear to extend far enough away from the springs to connect to other fault clusters, and therefore they likely play little role in determining regional groundwater flow paths. Perennial flow in the Verde River begins with a small spring discharging less than 0.1 m^3/s (5 ft^3/s) (Wirt et al., 2005), and it corresponds with the location of numerous faults, surrounding and including fault 60 (Figure 6B).

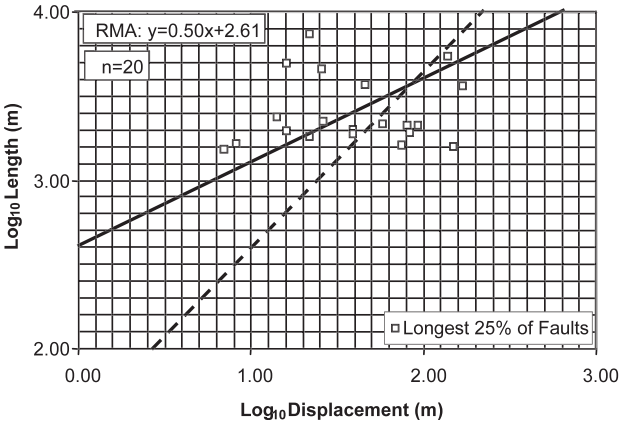

Figure 8. Log displacement versus log length of the longest 25 percent of faults in the Verde River headwaters. Note: Reduced major axis (solid line) slope is significantly less than the slope of the RMA calculated for the entire data set (dashed line).

CONCLUSIONS

We used fault scaling relations that are well known by structural geologists from brittle fault populations to better define a population of normal faults in north-central Arizona. By utilizing analytical methods in ArcGIS, statistical methods in Microsoft Excel, and field methods, including checking length and displacement of faults, a fault scaling relationship was determined specific to an extensional structural domain in the Transition Zone physiographic province of north-central Arizona. Through application of a fault scaling relationship where fault length and displacement have a linear relation, five faults with uncertain dimensions were identified as outliers, more accurately defined by analytical and field methods, and reassigned values closer to the expected value. This method of analyzing the fault population allowed for a better definition of the linkages between faults in the Verde River headwaters area, and a more thorough understanding of the hydrogeologic setting and processes of the region.

The methods we used are best applied to simple fault populations with mainly relatively short faults (few

kilometers and less) because longer faults may not follow the scaling relation as well due to incomplete fault linkages and complex growth histories. This method should be applicable to populations of faults of all types because the scaling relations have been found to apply universally (e.g., Schlische et al., 1996). This relatively simple length versus displacement relationship may be transferable to many other structural domains to assist with analyzing fault populations, the conceptualization of faults, and their simulation within framework and flow models. In simple structural domains, a modification of this method may be used when time only permits reconnaissance study of fault populations, wherein faults that form outliers are identified and queried in terms of their length or displacement. In these cases, one could judge if the outliers are important to investigate further depending on the goals of the study.

In general, isolated clusters of faults are present throughout the study area, but these clusters show no evidence of linkage to other clusters. Although locations of springs correlate to locations of faults, it appears that connectivity between faults plays only a small role in determining groundwater flow paths in the Verde River headwaters region.

ACKNOWLEDGMENTS

Major funding for the study was provided through the Arizona Department of Water Resources Water Protection Fund. Additional funding was provided by the Water Resources Research Center at the University of Arizona, Tucson, and the Watershed Research and Education Program at Northern Arizona University. We thank the reviewers for their valuable comments that improved the manuscript.

REFERENCES

Bailey, W. R.; Walsh, J. J.; and Manzocchi, T., 2005, Fault populations, strain distribution and basement fault reactivation in the East Pennies Coalfield, UK: *Journal Structural Geology*, Vol. 27, pp. 913–928.

Bense, V. F.; Van Balen, R. T.; and De Vries, J. J., 2003, The impact of faults on the hydrogeological conditions in the Roer Valley Rift system: An overview: *Netherlands Journal Geosciences*, Vol. 82, pp. 41–54.

Blasch, K. W.; Hoffman, J. P.; Graser, L. F.; Bryson, J. R.; and Flint, A. L., 2006, *Hydrogeology of the Upper and Middle Verde River Watersheds, Central Arizona*: U.S. Geological Survey Scientific Investigations Report 2005-5198. 101 p.

Bonnet, E.; Bour, O.; Odling, N. E.; Davy, P.; Main, I.; Cowie, P.; and Berkowitz, B., 2001, Scaling of fracture systems in geological media: *American Geophysical Union Reviews of Geophysics*, Vol. 39, pp. 347–383.

Bour, O. and Davy, P., 1997, Connectivity of random fault networks following a power law fault length distribution: *Water Resource Research*, Vol. 33, pp. 1567–1583.

Cartwright, J. A.; Trudgill, B. D.; and Mansfield, C. S., 1995, Fault growth by segment linkage: An explanation for scatter in maximum displacement and trace length data from the Canyonlands Grabens of SE Utah: *Journal Structural Geology*, Vol. 17, pp. 1319–1326.

Cook, P. G., 2003, *A Guide to Regional Groundwater Flow in Fractured Rock Aquifers: CSIRO Land and Water*: Seaview Press, Henley Beach, South Australia, 108 p.

Cowie, P. A. and Scholz, C. H., 1992a, Physical explanation for the displacement-length relationship of faults using a post-yield fracture mechanics model: *Journal Structural Geology*, Vol. 14, pp. 1133–1148.

Cowie, P. A. and Scholz, C. H., 1992b, Displacement-length scaling relationships for faults: Data synthesis and discussion: *Journal of Structural Geology*, Vol. 14, pp. 1149–1156.

Davis, G. H., 1978, Monocline fold pattern of the Colorado Plateau. In Matthews, V., III (Editor), *Laramide Folding Associated with Basement Block Faulting in the Western United States*: Geological Society of America Memoir 151, pp. 215–233.

Davis, J. C., 2002, *Statistics and Data Analysis in Geology,* 3rd ed.: John Wiley and Sons, New York.

DeWitt, E.; Langenheim, V. E.; and Wirt, L., 2005, Geologic framework. In Wirt, L.; DeWitt, E.; and Langenheim, V. E. (Editors), *Geologic Framework of Aquifer Units and Ground-Water Flowpaths, Verde River Headwaters, North-Central Arizona*: U.S. Geological Survey Open-File Report 2004-1411-B.

Dickinson, W. R., 1989, Tectonic setting of Arizona through geologic time. In Jenney, J. P. and Reynolds, S. J. (Editors), *Geologic Evolution of Arizona*: Arizona Geological Society Digest, Vol. 17, pp. 1–16.

Environmental Systems Research Institute, 2004, ArcGIS v. 9.1: Environmental Systems Research Institute Redlands, California.

Ferrill, D. A. and Morris, A. P., 2001, Displacement gradient and deformation in normal fault Systems: *Journal Structural Geology*, Vol. 23, pp. 619–638.

Gauthier, B. D. M. and Lake, S. D., 1993, Probabilistic modeling of faults below the limit of seismic resolution in Pelican Field, North Sea, Offshore United Kingdom: *American Association of Petroleum Geologists Bulletin*, Vol. 77, pp. 761–777.

Geocommunity website, 2006, Geocommunity website: Electronic document, available at http://www.geocomm.com

Gudmundsson, A., 2004, Effects of Young's modulus on fault displacement: *Geodynamics*, Vol. 336, pp. 85–92.

Hendricks, J. D. and Plescia, J. B., 1991, A review of the regional geophysics of the Arizona Transition Zone: *Journal of Geophysics Research*, Vol. 96, pp. 12351–12373.

Krieger, M. H., 1965, *Geology of the Prescott and Paulden Quadrangles, Arizona*: U.S. Geological Survey Professional Paper 467.

Mayer, J. R. and Sharp, J. M., Jr, 1998, Fracture control of regional ground-water flow in a carbonate aquifer in a semi-arid region: *Geological Society of America Bulletin*, Vol. 110, pp. 269–283.

Schlische, R. W.; Young, S. S.; Ackermann, R. V.; and Gupta, A., 1996, Geometry and scaling of a population of very small rift-related normal faults: *Geology*, Vol. 24, pp. 683–686.

Shipton, Z. K.; Evans, J. P.; and Thompson, L. B., 2005, The geometry and thickness of deformation-band fault core and its influence on sealing characteristics of deformation-band fault zones. In Sorkhabi, R. and Tsuji, Y. (Editors), *Faults,*

Fluid Flow, and Petroleum Traps: American Association of Petroleum Geologists Memoir 85, pp. 181–195.

Spencer, J. E. and Reynolds, S. J., 1989, Middle Tertiary tectonics of Arizona and adjacent areas. In Jenney, J. P. and Reynolds, S. J. (Editors), *Geologic evolution of Arizona*: Arizona Geological Society Digest 17, pp. 539–574.

Spencer, J. E.; Richards, S. M.; and Ferguson, C. A., 2001, Cenozoic structure and evolution of the boundary between the Basin and Range and Transition Zone provinces in Arizona. In Erskine, M. C.; Faulds, J. E.; Bartley, J. M.; and Rowley, P. D. (Editors), *The Geologic Transition, High Plateaus to Great Basin—A Symposium and Field Guide: The Mackin Volume*: Utah Geological Association Publication 30, pp. 239–271.

Walsh, J. J. and Watterson, J., 1988, Analysis of the relationship between displacement and dimensions of faults: *Journal Structural Geology*, Vol. 10, pp. 239–247.

Willemse, E. J. M.; Pollard, D. D.; and Aydin, A., 1996, Three-dimensional analysis of slip distributions on normal fault arrays with consequences for fault scaling: *Journal Structural Geology*, Vol. 18, pp. 295–309.

Wirt, L.; DeWitt, E.; and Langenheim, V. E., 2005, Hydrogeologic framework. In Wirt, L.; DeWitt, E.; and Langenheim, V. E. (Editors), *Geologic Framework of Aquifer Units and Ground-Water Flowpaths, Verde River Headwaters, North-Central Arizona*: U.S. Geological Survey Open-File Report 2004-1411-D.